

Specific heat and magnetic properties of $\text{Nd}_{0.5}\text{Sr}_{0.5}\text{MnO}_3$ and $\text{R}_{0.5}\text{Ca}_{0.5}\text{MnO}_3$ ($\text{R}=\text{Nd}, \text{Sm}, \text{Dy}, \text{and Ho}$)

J. López^{a)} and O. F. de Lima

Instituto de Física Gleb Wataghin, Universidade Estadual de Campinas, UNICAMP, 13083-970, Campinas, SP, Brazil

(Received 18 October 2002; accepted 15 July 2003)

Magnetization and specific heat measurements of $\text{Nd}_{0.5}\text{Sr}_{0.5}\text{MnO}_3$, $\text{Nd}_{0.5}\text{Ca}_{0.5}\text{MnO}_3$, $\text{Sm}_{0.5}\text{Ca}_{0.5}\text{MnO}_3$, $\text{Dy}_{0.5}\text{Ca}_{0.5}\text{MnO}_3$, and $\text{Ho}_{0.5}\text{Ca}_{0.5}\text{MnO}_3$ samples were performed. Near the charge ordering (CO) and ferromagnetic transition temperatures, the specific heat curves showed peaks superimposed to the characteristic response of the lattice oscillations. These peaks allowed us to estimate the entropy variation for each phase transition. The entropy variation corresponding to the CO transition was higher than the one corresponding to the ferromagnetic transition. Furthermore, specific heat measurements in presence of a 9 T magnetic field showed that this field was not strong enough to affect the specific heat in the CO phase transition region. Our results suggest that the CO phase is very stable and almost independent of magnetic fields. © 2003 American Institute of Physics. [DOI: 10.1063/1.1606517]

I. INTRODUCTION

The physical properties in charge ordering (CO) manganese perovskites are considered to arise from the strong competition involving a ferromagnetic double-exchange interaction, an antiferromagnetic superexchange interaction, and the spin-phonon coupling.¹⁻⁷ These interactions are determined by intrinsic parameters such as doping level, average cationic size, cationic disorder, and oxygen stoichiometry. CO compounds are particularly interesting because spin, charge, and orbital degrees of freedom are at play simultaneously and classical simplifications, that neglect some of these interactions, are not valid. More detailed information on the physics of manganites can be found in a review paper by Salamon and Jaime.⁸

The specific heat at low temperature, for $\text{LaMnO}_{3+\delta}$ samples, was found by Ghivelder *et al.*⁹ to be very sensitive to small variations of δ , similar to results published by Schnelle *et al.*¹⁰ in a $\text{Nd}_{0.67}\text{Sr}_{0.33}\text{MnO}_{3-\delta}$ sample. In this latter work, and also in a paper by Gordon *et al.*,¹¹ a Schottky-type anomaly was found at low temperatures. They associated this result with the magnetic ordering of Nd^{3+} ions and to the crystal-field splitting. Bartolomé *et al.*¹² also found a Schottky-type anomaly in a closely related compound of NdCrO_3 . They proposed a crystal-field energy level scheme in agreement with neutron-scattering studies in the same sample. In a series of two papers, Smolyaninova *et al.*^{13,14} studied the low-temperature specific heat in $\text{Pr}_{1-x}\text{Ca}_x\text{MnO}_3$ ($0.3 < x < 0.5$) and $\text{La}_{1-x}\text{Ca}_x\text{MnO}_3$ ($x=0.47, 0.5, \text{and } 0.53$). They fitted the data with an excess specific heat, $C'(T)$, of nonmagnetic origin associated with CO. They also showed that a magnetic field, sufficiently high to induce a transition from the charge ordered state to the ferromagnetic metallic state, did not completely remove $C'(T)$. However, no Schottky anomaly was found in any of these compounds.

We have already presented specific heat measurements with applied magnetic fields between 0 and 9 T and temperatures between 2 and 30 K for $\text{Nd}_{0.5}\text{Sr}_{0.5}\text{MnO}_3$, $\text{Nd}_{0.5}\text{Ca}_{0.5}\text{MnO}_3$, $\text{Sm}_{0.5}\text{Ca}_{0.5}\text{MnO}_3$, $\text{Dy}_{0.5}\text{Ca}_{0.5}\text{MnO}_3$, and $\text{Ho}_{0.5}\text{Ca}_{0.5}\text{MnO}_3$ samples. All of these compounds presented a Schottky-type anomaly at low temperatures.^{15,16} Here, we report a general magnetic characterization and specific heat measurements in the full temperature interval, between 2 and 300 K, for the same five samples.

II. EXPERIMENTAL METHODS

Polycrystalline samples of $\text{Nd}_{0.5}\text{Sr}_{0.5}\text{MnO}_3$, $\text{Nd}_{0.5}\text{Ca}_{0.5}\text{MnO}_3$, and $\text{Ho}_{0.5}\text{Ca}_{0.5}\text{MnO}_3$ were prepared by the sol-gel method.¹⁷ Stoichiometric parts of Nd_2O_3 (Ho_2O_3) and MnCO_3 were dissolved in HNO_3 and mixed to an aqueous citric acid solution, to which SrCO_3 or CaCO_3 was added. The mixed metallic citrate solution presented the ratio citric acid/metal of 1/3 (in molar basis). Ethylene glycol was added to this solution, to obtain a citric acid/ethylene glycol ratio 60/40 (mass ratio). The resulting solution was neutralized to a $\text{pH}\sim 7$ with ethylenediamine. This solution was turned into a gel, and subsequently decomposed to a solid by heating at 400 °C. The resulting powder was heat treated in a vacuum at 900 °C for 24 h, with several intermediary grindings, in order to prevent formation of impurity phases. This powder was pressed into pellets and sintered in air at 1050 °C for 12 h.

Polycrystalline samples of $\text{Sm}_{0.5}\text{Ca}_{0.5}\text{MnO}_3$ and $\text{Dy}_{0.5}\text{Ca}_{0.5}\text{MnO}_3$ were prepared from stoichiometric amounts of Sm_2O_3 or Dy_2O_3 , CaO , and MnO_2 by a standard solid-state reaction method. All of the powders were mixed and ground for a long time in order to produce a homogeneous mixture. First, the mixture was heated at 927 °C for 24 h and, after that, it was ground and heated at 1327 °C (72 h) and 1527 °C (48 h). X-ray diffraction measurements indicated high-quality samples in all cases.

^{a)}Electronic mail: jlopezlb@yahoo.com.br

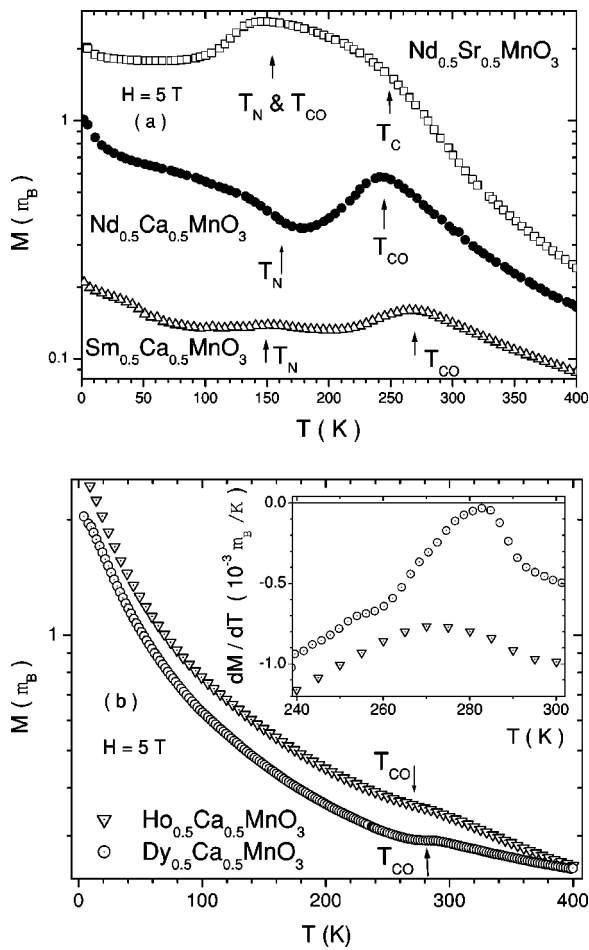


FIG. 1. Temperature dependence of the magnetization, with a 5 T applied magnetic field, in field-cooling–warming condition for the five polycrystalline samples studied. Magnetization is given in Bohr magnetons per manganese ion. The Curie (T_C), Néel (T_N) and CO (T_{CO}) temperatures are indicated for each curve. The curves are plotted in a semilogarithmic scale to allow the comparison of all samples. The inset in (b) represents the temperature derivative of the magnetization near the charge ordering transition.

The magnetization measurements were done with a Quantum Design MPMS-5S superconducting quantum interference device magnetometer. Specific heat measurements were made with a Quantum Design PPMS calorimeter that uses a *two-relaxation time* technique, and data were always collected during sample cooling. The intensity of the heat pulse was calculated to produce a variation in the temperature bath between 0.5% (at low temperatures) and 2% (at high temperatures). Experimental errors during the specific heat and magnetization measurements were lower than 1% for all temperatures and samples.

III. RESULTS AND DISCUSSION

A. Magnetization measurements

Figure 1 shows the temperature dependence of magnetization, measured for all of the studied samples, with an applied magnetic field of 5 T and using a field-cooling condition. The results are presented in a semilogarithmic scale to facilitate comparisons. CO transition temperatures (T_{CO}) are indicated by arrows in Fig. 1 at 160, 250, 270, 280, and 271

K, respectively. These temperatures are associated with peaks in the magnetization curves, in agreement with previous reports.^{18–21} It is interesting to note that the relation between the CO temperature and the antiferromagnetic ordering temperature (T_N) changes for each sample.^{18–21} For $Nd_{0.5}Sr_{0.5}MnO_3$, we found $T_{CO} \approx T_N$, for $Nd_{0.5}Ca_{0.5}MnO_3$ and $Sm_{0.5}Ca_{0.5}MnO_3$, we found $T_{CO} \gg T_N$, and for $Dy_{0.5}Ca_{0.5}MnO_3$ and $Ho_{0.5}Ca_{0.5}MnO_3$; a long-range antiferromagnetic transition was not observed.

The $Nd_{0.5}Sr_{0.5}MnO_3$ sample presented a ferromagnetic transition at $T_C \approx 244$ K and an antiferromagnetic transition at $T_N \approx 160$ K. The $Nd_{0.5}Ca_{0.5}MnO_3$ compound presented a strong magnetization maximum near T_{CO} , but showed an unexpected minimum close to $T_N = 160$ K, where a maximum would be usually found. The antiferromagnetic transition in $Sm_{0.5}Ca_{0.5}MnO_3$ presented a maximum at $T_N \approx 150$ K. For temperatures lower than 10, 20, and 50 K, the $Nd_{0.5}Sr_{0.5}MnO_3$, $Nd_{0.5}Ca_{0.5}MnO_3$, and $Sm_{0.5}Ca_{0.5}MnO_3$ samples, respectively, showed a sharp increase in the magnetization. This trend has been associated with a short-range magnetic ordering of the intrinsic magnetic moment of Nd^{3+} ions.²² However, no long-range ferromagnetic order of the Nd^{3+} ions was found in neutron diffraction measurements at these low temperatures.^{18,19}

Different from the three previous samples, the $Dy_{0.5}Ca_{0.5}MnO_3$ and $Ho_{0.5}Ca_{0.5}MnO_3$ compounds do not present a strong magnetization maximum at the CO temperature. However, a clear inflection is observed at T_{CO} for both samples, as revealed by the temperature derivative in the inset of Fig. 1(b). The existence of CO in $Dy_{0.5}Ca_{0.5}MnO_3$ and $Ho_{0.5}Ca_{0.5}MnO_3$ was suggested by Terai *et al.*²¹ after studies of magnetization and resistivity curves. As shown ahead, our specific heat measurements present peaks close to the same temperature interval of the suggested charge ordered transition.

B. Specific heat at high temperatures

Figure 2 shows specific heat measurements with a zero-applied magnetic field from 2 to 300 K in the $Nd_{0.5}Sr_{0.5}MnO_3$, $Nd_{0.5}Ca_{0.5}MnO_3$, $Sm_{0.5}Ca_{0.5}MnO_3$, $Dy_{0.5}Ca_{0.5}MnO_3$, and $Ho_{0.5}Ca_{0.5}MnO_3$ samples. In order to facilitate the visualization, the curves for $Nd_{0.5}Sr_{0.5}MnO_3$ and $Ho_{0.5}Ca_{0.5}MnO_3$ were displaced 20 J/mol K upside and downside in Fig. 2(a), and the curve for $Dy_{0.5}Ca_{0.5}MnO_3$ was displaced 20 J/mol K downside in Fig. 2(b). Specific heat measurements give information about both lattice and magnetic excitations. At high temperatures, the excitations from the lattice vibrations are dominant and decrease as the temperature decreases. The magnetic contribution can be obtained approximately by subtracting the lattice part from the experimental values.

Continuous lines in Fig. 2 represent the fitting of the thermal background, in the interval from 30 K to 300 K, using the Einstein given by

$$C_{\text{Einstein}} = 3nR \sum_i a_i \left[\frac{x_i^2 e^{x_i}}{(e^{x_i} - 1)^2} \right], \quad (1)$$

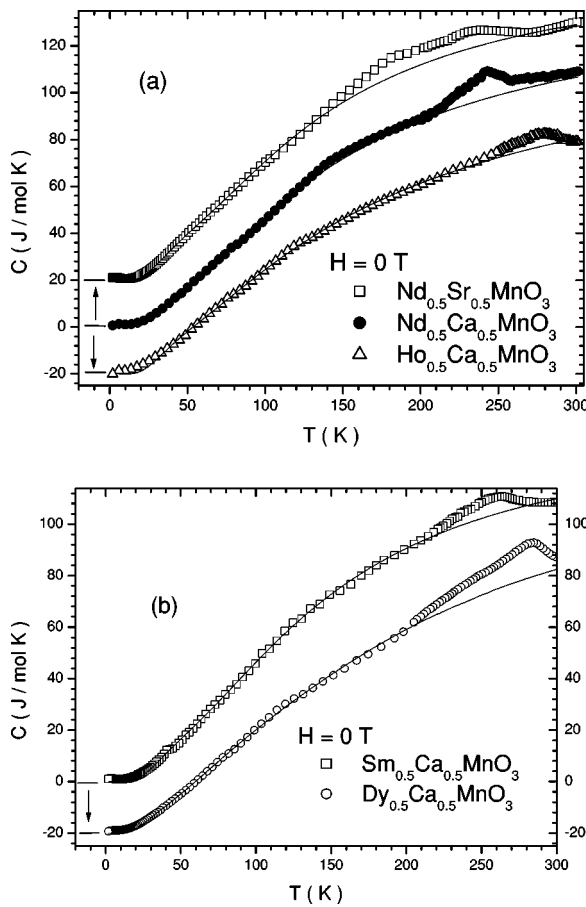


FIG. 2. Specific heat measurements between 2 and 300 K in the five measured samples. Continuous lines represent the fitting of the phonon background to the Einstein model. The $\text{Nd}_{0.5}\text{Sr}_{0.5}\text{MnO}_3$ and $\text{Ho}_{0.5}\text{Ca}_{0.5}\text{MnO}_3$ curves in (a) were displaced 20 J/mol K upside and downside, respectively; the $\text{Ho}_{0.5}\text{Ca}_{0.5}\text{MnO}_3$ curve in (b) was displaced 20 J/mol K downside.

where $x_i = T_i/T$. Three optical phonons ($i = 1, 2, 3$) with energies T_i (in Kelvin) and relative occupations a_i were used. The Einstein model for the specific heat considers the oscillation frequency (or energy) independent of the wave vector, which is a valid approximation for the optical part of the spectrum. The values of temperatures (energies) and relative occupations are shown in Table I. These values are similar to those reported, using the same model, by Ramirez *et al.*²³ in a $\text{La}_{0.37}\text{Ca}_{0.63}\text{MnO}_3$ sample and Raychaudhuri *et al.*²⁴ in a $\text{Pr}_{0.63}\text{Ca}_{0.37}\text{MnO}_3$ sample. However, we should point out that the values found are not unique since there are six free parameters during the fitting (one energy and one occupation coefficient for each oscillation mode). The thermal back-

TABLE I. Values of energies T_i (in Kelvin) and relative occupations a_i for the three optical phonons ($i = 1, 2, 3$) in an Einstein model for the specific heat in all the studied samples.

Sample	T_1 (K)	T_2 (K)	T_3 (K)	a_1	a_2	a_3
$\text{Nd}_{0.5}\text{Sr}_{0.5}\text{MnO}_3$	148	438	997	0.30	0.64	0.11
$\text{Nd}_{0.5}\text{Ca}_{0.5}\text{MnO}_3$	152	432	1035	0.27	0.62	0.18
$\text{Sm}_{0.5}\text{Ca}_{0.5}\text{MnO}_3$	157	450	846	0.27	0.64	0.16
$\text{Dy}_{0.5}\text{Ca}_{0.5}\text{MnO}_3$	126	351	821	0.17	0.41	0.51
$\text{Ho}_{0.5}\text{Ca}_{0.5}\text{MnO}_3$	147	438	1023	0.27	0.51	0.25

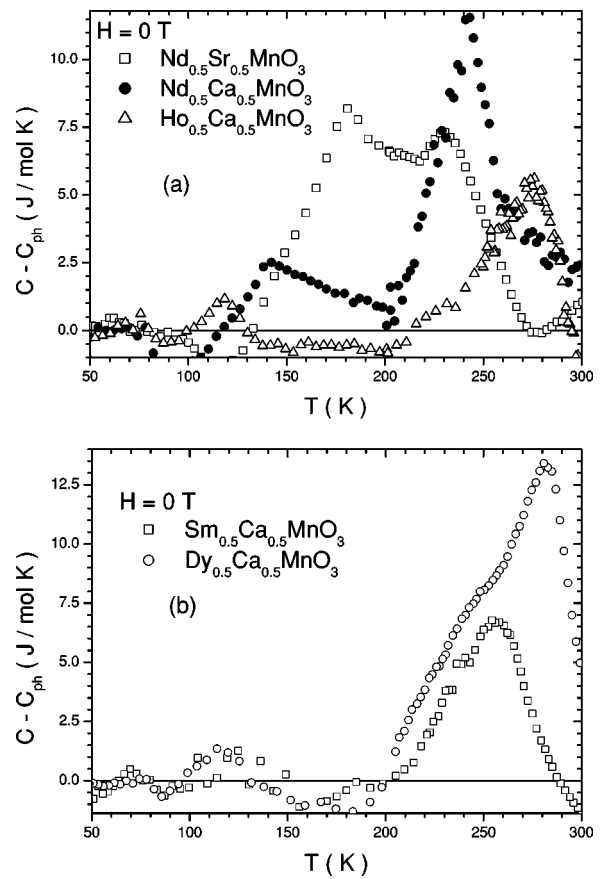


FIG. 3. Differences between the experimental specific heat data and the corresponding background curves in $\text{Nd}_{0.5}\text{Sr}_{0.5}\text{MnO}_3$, $\text{Nd}_{0.5}\text{Ca}_{0.5}\text{MnO}_3$, $\text{Sm}_{0.5}\text{Ca}_{0.5}\text{MnO}_3$, $\text{Dy}_{0.5}\text{Ca}_{0.5}\text{MnO}_3$, and $\text{Ho}_{0.5}\text{Ca}_{0.5}\text{MnO}_3$ samples.

ground determination is particularly risky, because it could have also a “tail” due to any magnetic or CO anomaly. Nonetheless, this seems to be one of the best possible methods to quantify the specific heat at high temperatures.

Figure 3 represents the differences between the experimental data and the fitted curves in Fig. 2. There is a maximum at 231 K for the $\text{Nd}_{0.5}\text{Sr}_{0.5}\text{MnO}_3$ sample, which is correlated with the ferromagnetic transition at 250 K in the corresponding magnetization curve (Fig. 1). A second maximum, which could be partially associated with the antiferromagnetic and CO transitions at 160 K, appears at 180 K. However, the lattice parameters in this compound change rapidly between approximately 110 K and 250 K.²⁵ The variation in lattice parameters affects the strength of the interactions between the atoms and the phonons frequency, contributing to the specific heat in the second peak.

Figure 3 also shows that there is a maximum at 243 K for the $\text{Nd}_{0.5}\text{Ca}_{0.5}\text{MnO}_3$ sample. This maximum correlates with the corresponding CO temperature at 250 K. Different from the $\text{Nd}_{0.5}\text{Sr}_{0.5}\text{MnO}_3$ compound, there is no magnetic ordering in this high-temperature interval for the $\text{Nd}_{0.5}\text{Ca}_{0.5}\text{MnO}_3$ sample. However, in the latter case, the lattice parameters change very rapidly between approximately 200 K and 250 K.¹⁹ An inflection point in the C versus T curve [Fig. 2(a)] appears at 141 K for the $\text{Nd}_{0.5}\text{Ca}_{0.5}\text{MnO}_3$ sample. Besides, there is a maximum at 141 K in Fig. 3, but its height is relatively small compared to the maximum at

243 K. The Néel temperature corresponding to this compound is 160 K. Therefore, these results lead us to conclude that the specific heat variations due to the antiferromagnetic order are small compared to those induced by the CO and ferromagnetic transitions.

For the $\text{Sm}_{0.5}\text{Ca}_{0.5}\text{MnO}_3$, $\text{Dy}_{0.5}\text{Ca}_{0.5}\text{MnO}_3$, and $\text{Ho}_{0.5}\text{Ca}_{0.5}\text{MnO}_3$ samples, the maxima were found at 254 K, 281 K, and 276 K, respectively. These experimental results and the resistivity measurements reported by Tokura *et al.*²⁰ and Terai *et al.*,²¹ are strong evidence that indicate the existence of CO transitions in the $\text{Sm}_{0.5}\text{Ca}_{0.5}\text{MnO}_3$, $\text{Dy}_{0.5}\text{Ca}_{0.5}\text{MnO}_3$, and $\text{Ho}_{0.5}\text{Ca}_{0.5}\text{MnO}_3$ samples. However, electron diffraction studies would be needed to unambiguously classify this transition as CO. The other small peaks, which are comparable to the experimental error, could not be correlated to any magnetic transition.

Results in Fig. 3 allow us to calculate the variation in entropy (ΔS), within the limits of the model, associated with the CO, ferromagnetic, and antiferromagnetic transitions:

$$\Delta S = \int_{T_i}^{T_f} \frac{(C - C_{\text{ph}})}{T} dT, \quad (2)$$

where T_i and T_f are two temperatures conveniently chosen to delineate the interval of interest and C_{ph} is the specific heat due to the phonons.

For the $\text{Nd}_{0.5}\text{Ca}_{0.5}\text{MnO}_3$ sample, the entropy variation between 201 and 301 K, with $H=0$, was $\Delta S(T_{\text{CO}}) = 2.0 \text{ J}/(\text{mol K})$. Raychaudhuri *et al.*²⁴ reported an entropy variation, close to the CO transition in the compound $\text{Pr}_{0.63}\text{Ca}_{0.37}\text{MnO}_3$, of $1.8 \text{ J}/(\text{mol K})$ with zero-applied magnetic field and $1.5 \text{ J}/(\text{mol K})$ with an 8 T magnetic field. On the other hand, Ramirez *et al.*²³ found $\Delta S(T_{\text{CO}}) = 5 \text{ J}/(\text{mol K})$ in a $\text{La}_{0.37}\text{Ca}_{0.63}\text{MnO}_3$ sample. All of these results correspond to those expected for a CO transition.²⁴ Besides, the entropy variation (not related to phonons), calculated between 118 K and 201 K for the $\text{Nd}_{0.5}\text{Ca}_{0.5}\text{MnO}_3$ sample, $\Delta S(T_N) = 0.80 \text{ J}/(\text{mol K})$. We associate this smaller ΔS value to the antiferromagnetic order occurring at $T_N = 160 \text{ K}$.

The entropy variation between 133 K and 274 K for the $\text{Nd}_{0.5}\text{Sr}_{0.5}\text{MnO}_3$ sample was $\Delta S(T_{\text{CO+FM}}) = 3.6 \text{ J}/(\text{mol K})$. Considering that the entropy variation associated with the CO transition is the same as for the $\text{Nd}_{0.5}\text{Ca}_{0.5}\text{MnO}_3$ sample, one finds that the entropy variation associated with the ferromagnetic transition is approximately $1.6 \text{ J}/(\text{mol K})$. Using a model proposed by Gordon *et al.*,¹¹ we estimate that the change in entropy needed to produce a full ferromagnetic transition in the $\text{Nd}_{0.5}\text{Sr}_{0.5}\text{MnO}_3$ sample would be $12.45 \text{ J}/(\text{mol K})$. Therefore, the fact that the entropy variation found is 13% of the theoretical value suggests that only a small part of the spins order ferromagnetically. Gordon *et al.*¹¹ found also that the entropy variation associated with the ferromagnetic order in a $\text{Nd}_{0.67}\text{Sr}_{0.33}\text{MnO}_3$ sample was approximately 10% of the theoretical value. The entropy variations, not associated with lattice oscillations, between 200 K and 300 K, for the $\text{Sm}_{0.5}\text{Ca}_{0.5}\text{MnO}_3$ and $\text{Dy}_{0.5}\text{Ca}_{0.5}\text{MnO}_3$ samples were $\Delta S(T_{\text{CO}}) = 1.15 \text{ J}/(\text{mol K})$ and $2.80 \text{ J}/(\text{mol K})$. Between 216 K and 294 K, for the $\text{Ho}_{0.5}\text{Ca}_{0.5}\text{MnO}_3$ sample, it was found $\Delta S(T_{\text{CO}}) = 0.78 \text{ J}/(\text{mol K})$. The entropy variations for

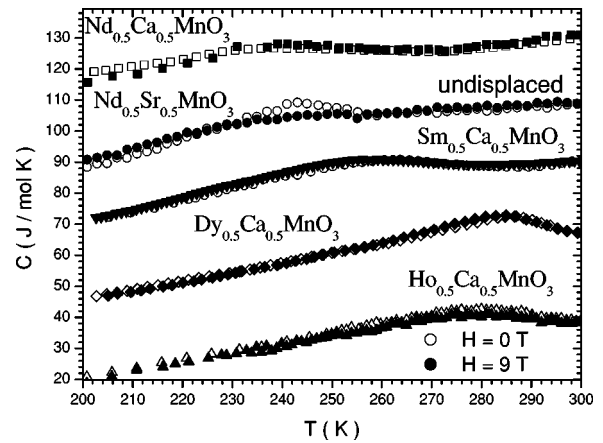


FIG. 4. Specific heat measurements between 200 and 300 K with a zero-applied magnetic field (open symbols) and with $H=9 \text{ T}$ (closed symbols) in the five measured samples. To allow comparisons, the $\text{Nd}_{0.5}\text{Ca}_{0.5}\text{MnO}_3$ curve was displaced 20 J/mol K upside; the $\text{Sm}_{0.5}\text{Ca}_{0.5}\text{MnO}_3$, $\text{Dy}_{0.5}\text{Ca}_{0.5}\text{MnO}_3$, and $\text{Ho}_{0.5}\text{Ca}_{0.5}\text{MnO}_3$ curves were displaced 20, 40, and 60 J/mol K downside, respectively.

$\text{Sm}_{0.5}\text{Ca}_{0.5}\text{MnO}_3$ and $\text{Dy}_{0.5}\text{Ca}_{0.5}\text{MnO}_3$ are closer to the one for the $\text{Nd}_{0.5}\text{Ca}_{0.5}\text{MnO}_3$ sample. The $\Delta S(T_{\text{CO}})$ for the $\text{Ho}_{0.5}\text{Ca}_{0.5}\text{MnO}_3$ sample is smaller than for the other samples, suggesting a different nature of the CO transition in this compound.

Figure 4 shows the specific heat measurements, between 200 and 300 K, with a zero-applied magnetic field (open symbols) and with $H=9 \text{ T}$ (closed symbols) for the five measured samples. To allow comparisons, the $\text{Nd}_{0.5}\text{Ca}_{0.5}\text{MnO}_3$ curve was displaced 20 J/mol K upside; the $\text{Sm}_{0.5}\text{Ca}_{0.5}\text{MnO}_3$, $\text{Dy}_{0.5}\text{Ca}_{0.5}\text{MnO}_3$, and $\text{Ho}_{0.5}\text{Ca}_{0.5}\text{MnO}_3$ curves were displaced 20, 40, and 60 J/mol K downside, respectively. The external magnetic field suppresses the peak around the ferromagnetic temperature in the $\text{Nd}_{0.5}\text{Sr}_{0.5}\text{MnO}_3$ sample. Although a 9 T magnetic field is much smaller than the thermodynamic field given by $k_B T_C / \mu_B$, near the ferromagnetic phase transition, the system is in an unstable condition, which is very sensitive to the external magnetic field. This fact explains the suppression of the peak in the presence of the field in the specific heat curve and the decrease in the slope of the magnetization curve (not shown). On the other hand, the external magnetic field seems to have no effect on the specific heat of the other four compounds. This result indicates that, although the sample magnetization increases with temperature close to the CO transition, the CO phase does not appear to depend on the application of an external magnetic field. Indeed, our experiments show that an external magnetic field of 9 T is not strong enough to produce variations in the specific heat of the CO phase occurring in these samples. On the other hand, the increase of magnetization close to T_{CO} is associated with an abrupt change in lattice parameters²⁰ that affects the distance among magnetic ions and, hence, their interactions.

IV. CONCLUSIONS

We have made a magnetic characterization of $\text{Nd}_{0.5}\text{Sr}_{0.5}\text{MnO}_3$, $\text{Nd}_{0.5}\text{Ca}_{0.5}\text{MnO}_3$, $\text{Sm}_{0.5}\text{Ca}_{0.5}\text{MnO}_3$,

$Dy_{0.5}Ca_{0.5}MnO_3$, and $Ho_{0.5}Ca_{0.5}MnO_3$ polycrystalline samples. Ferromagnetic, antiferromagnetic, and CO transitions in our samples agreed with previous reports. We also reported specific heat measurements with applied magnetic fields between 0 and 9 T and temperatures between 2 and 300 K in all the five samples. Each curve was fitted at high temperatures by an Einstein model with three optical phonon modes. Close to the CO and ferromagnetic transition temperatures, the specific heat curves showed peaks superimposed on the characteristic response of the lattice oscillations. The entropy variation corresponding to the CO transition was higher than the one corresponding to the ferromagnetic transition. Near 160 K, the specific heat curves showed an abrupt change in slope for the two compounds with Nd^{3+} ions, which were correlated with the corresponding antiferromagnetic transition. However, an external 9 T magnetic field seems to have no effect in the specific heat of the CO phase transition.

ACKNOWLEDGMENTS

The authors thank Dr. P. N. Lisboa-Filho for the preparation of $Nd_{0.5}Sr_{0.5}MnO_3$, $Nd_{0.5}Ca_{0.5}MnO_3$, and $Ho_{0.5}Ca_{0.5}MnO_3$ samples and the Brazilian science agencies FAPESP and CNPq for the financial support.

¹P. G. Radaelli, D. E. Cox, M. Marezio, and S.-W. Cheong, *Phys. Rev. B* **55**, 3015 (1997).

²G. Zhao, K. Ghosh, and R. L. Greene, *J. Phys.: Condens. Matter* **10**, L737 (1998).

³Y. Moritomo, *Phys. Rev. B* **60**, 10374 (1999).

⁴G. Xiao, G. Q. Gong, C. L. Canedy, E. J. McNiff, Jr., and A. Gupta, *J. Appl. Phys.* **81**, 5324 (1997).

⁵S. Mori, C. H. Chen, and S.-W. Cheong, *Nature (London)* **392**, 473 (1998).

⁶J. López, P. N. Lisboa-Filho, W. A. C. Passos, W. A. Ortiz, and F. M.

Araujo-Moreira, *J. Magn. Magn. Mater.* **226**, 507 (2001); also at <http://arxiv.org/abs/cond-mat/0004460>

⁷J. López, P. N. Lisboa Filho, W. A. C. Passos, W. A. Ortiz, F. M. Araujo-Moreira, K. Ghosh, O. F. de Lima, and D. Schaniel, *Phys. Rev. B* **63**, 224422 (2001); also at <http://arxiv.org/abs/cond-mat/0103305>

⁸M. B. Salamon and M. Jaime, *Rev. Mod. Phys.* **73**, 583 (2001).

⁹L. Ghivelder, I. Abrego Castillo, M. A. Gusmão, J. A. Alonso, and L. F. Cohen, *Phys. Rev. B* **60**, 12184 (1999).

¹⁰W. Schnelle, A. Poddar, P. Murugaraj, E. Gmelin, R. K. Kremer, K. Sasaki, and J. Maier, *J. Phys.: Condens. Matter* **12**, 4001 (2000).

¹¹J. E. Gordon, R. A. Fisher, Y. X. Jia, N. E. Phillips, S. F. Reklis, D. A. Wright, and A. Zettl, *Phys. Rev. B* **59**, 127 (1999).

¹²F. Bartolomé, J. Bartolomé, M. Castro, and J. J. Melero, *Phys. Rev. B* **62**, 1058 (2000).

¹³V. N. Smolyaninova, K. Ghosh, and R. L. Greene, *Phys. Rev. B* **58**, R14725 (1998).

¹⁴V. N. Smolyaninova, Amlan Biswas, X. Zhang, K. H. Kim, B.-G. Kim, S.-W. Cheong, and R. L. Greene, *Phys. Rev. B* **62**, R6093 (2000).

¹⁵J. López, P. N. Lisboa-Filho, O. F. de Lima, and F. M. Araujo-Moreira, *J. Magn. Magn. Mater.* **242**, 683 (2002); also at <http://arxiv.org/abs/cond-mat/0105571>

¹⁶J. López, P. N. Lisboa-Filho, O. F. de Lima, and F. M. Araujo-Moreira, *Phys. Rev. B* **66**, 214402 (2002); also at <http://arxiv.org/abs/cond-mat/0208381>

¹⁷L. Filho, P. N. , S. M. Zanetti, E. R. Leite, and W. A. Ortiz, *Mater. Lett.* **38**, 289 (1999).

¹⁸R. Kajimoto, H. Yoshizawa, H. Kawano, H. Kuwahara, Y. Tokura, K. Ohoyama, and M. Ohashi, *Phys. Rev. B* **60**, 9506 (1999).

¹⁹F. Millange, S. de Brion, and G. Chouteau, *Phys. Rev. B* **62**, 5619 (2000).

²⁰Y. Tokura and Y. Tomioka, *J. Magn. Magn. Mater.* **200**, 1 (1999).

²¹T. Terai, T. Sasaki, T. Kakeshita, T. Fukuda, T. Saburi, H. Kitagawa, K. Kindo, and M. Honda, *Phys. Rev. B* **61**, 3488 (2001).

²²R. Mathieu, P. Nordblad, A. R. Raju, and C. N. R. Rao, <http://arxiv.org/abs/cond-mat/0106606> (2001).

²³A. P. Ramirez, P. Schiffer, S.-W. Cheong, C. H. Chen, W. Bao, T. T. M. Palstra, P. L. Gammel, D. J. Bishop, and B. Zegarski, *Phys. Rev. Lett.* **76**, 3188 (1996).

²⁴A. K. Raychaudhuri, A. Guha, I. Das, R. Rawat, and C. N. R. Rao, *Phys. Rev. B* **64**, 165111 (2001).

²⁵S. Shimomura, K. Tajima, N. Wakabayashi, S. Kobayashi, H. Kuwahara, and Y. Tokura, *J. Phys. Soc. Jpn.* **68**, 1943 (1999).